In Situ Calorimetric Study of the Growth of Silica TPA-MFI Crystals from an Initially Clear Solution

Sanyuan Yang and Alexandra Navrotsky*

Thermochemistry Facility, Department of Chemical Engineering and Materials Science, University of California at Davis, Davis, California 95616

Received February 5, 2002. Revised Manuscript Received April 15, 2002

Direct evidence from in situ calorimetric experiments demonstrates that the crystal growth of silica TPA-MFI zeolite (TPA = tetrapropylammonium, MFI = framework structure code of ZSM-5) at 95 °C from an initially clear solution ($9.00TPAOH-25.0SiO_2-480.0H_2O-100.0C_2H_5OH$) is first exothermic and then endothermic. The distinct exo → endo thermal switch coincides with a sharp pH rise of the mother liquor from 12.6 to 13.3. The crystal growth in the exothermic stage is driven by a constant enthalpy release of -0.514 ± 0.014 kJ/mol of SiO_2. The accumulated crystal mass is consistent with a rate of crystal growth that is linear with time and with the integral enthalpy change. In the endothermic stage of growth, the energetic driving force diminishes quickly and an increasing energetic hindering force ensues, about 2.5 kJ/mol of SiO_2 near the end of the reaction. Crystal growth under an energetic hindering force implies an entropic driving force, which is mainly attributed to the liberation of small chemical species such as OH^- and/or H_2O into solution from the eliminated interface. The results are discussed on the basis of a crystal growth mechanism of orderly aggregation of the preassembled primary TPA-MFI particles about 3 nm in diameter formed in the initial solution. Because of the small size and large specific surface area of the particles involved in the crystal growth, the crystal growth results in significant reduction of the overall interface between the solid particles and mother liquor. In the exothermic stage of growth, the constant solution pH indicates that the surface charge on the eliminated interface is compressed onto the remaining interface via deprotonation of the silanols there. However, in the endothermic stage, the rapid increase of the solution pH suggests that further compression of the surface charge by crystal growth apparently becomes energetically prohibited so that releasing OH^- into solution prevails. In much of the crystal growth period, the reaction rate is controlled by surface reaction kinetics. Only when approaching the end of crystal growth does the energetic hindering force become so significant that the thermodynamics gradually dominates the reaction process and finally terminates the reaction.

Introduction

Aggregation of nanocrystals results not only in disordered solids but also in oriented macrocrystals.[1] Kajiwara et al. found that a large number of nanocrystals in the aggregate formed from sputter-deposited amorphous Ti-rich Ti−Ni thin films have exactly the same orientation.[2] Banfield et al. proposed a mechanism of "oriented-attachment" of primary particles with diameters of 2−3 nm in the biomineralization of iron oxyhydroxide.[3] In the synthesis of silica TPA-MFI zeolite (TPA = tetrapropylammonium, MFI = framework structure code of ZSM-5), many researchers have reported the existence of preassembled primary particles (PPs) about 3 nm in diameter.[4−16] These primary particles, with compositional and structural features similar to those of the bulk crystals, aggregate into highly ordered extended structures by an addition mechanism.[5,6,11,16]

* Corresponding author. Fax: (530) 752-9307. E-mail: anavrotsky@ucdavis.edu.

(1) Alivisatos, A. P. *Science (Washington, D. C.)* **2000**, *289*, 736.
(2) Kajiwara, S.; Ogawa, K.; Kikuchi, T.; Matsunaga, T.; Miyazaki, S. *Philos. Mag. Lett.* **1996**, *74*, 395.
(3) Banfield, J. F.; Welch, S. A.; Zhang, H.; Ebert, T. T.; Penn, R. L. *Science* (*Washington, D. C.*) **2000**, *289*, 751.
(4) Schoeman, B. J. *Zeolites* **1997**, *18*, 97.
(5) Kirschhock, C. E. A.; Ravishankar, R.; Jacobs, P. A.; Martens, J. A. *J. Phys. Chem. B* **1999**, *103*, 11021.
(6) De Moor, P.-P. E. A.; Beelen, T. P. M.; Komanschek, B. U.; Beck, L. W.; Wagner, P.; Davis, M. E.; Van Santen, R. A. *Chem.—Eur. J.* **1999**, *5*, 2083.
(7) Kirschhock, C. E. A.; Ravishankar, R.; Van Looveren, L.; Jacobs, P. A.; Martens, J. A. *J. Phys. Chem. B* **1999**, *103*, 4972.
(8) Kirschhock, C. E. A.; Ravishankar, R.; Verspeurt, F.; Grobet, P. J.; Jacobs, P. A.; Martens, J. A. *J. Phys. Chem. B* **1999**, *103*, 4965.
(9) Ravishankar, R.; Kirschhock, C. E. A.; Knops-Gerrits, P.-P.; Feijen, E. J. P.; Grobet, P. J.; Vanoppen, P.; De Schryver, F. C.; Miehe, G.; Fuess, H.; Schoeman, B. J.; Jacobs, P. A.; Martens, J. A. *J. Phys. Chem. B* **1999**, *103*, 4960.
(10) Ravishankar, R.; Kirschhock, C.; Schoeman, B. J.; Vanoppen, P.; Grobet, P. J.; Storck, S.; Maier, W. F.; Martens, J. A.; De Schryver, F. C.; Jacobs, P. A. *J. Phys. Chem. B* **1998**, *102*, 2633.
(11) Nikolakis, V.; Kokkoli, E.; Tirrell, M.; Tsapatsis, M.; Vlachos, D. G. *Chem. Mater.* **2000**, *12*, 845.
(12) Watson, J. N.; Iton, L. E.; Keir, R. I.; Thomas, J. C.; Dowling, T. L.; White, J. W. *J. Phys. Chem. B* **1997**, *101*, 10094.
(13) De Moor, P.-P. E. A.; Beelen, T. P. M.; Van Santen, R. A. *J. Phys. Chem. B* **1999**, *103*, 1639.
(14) Schoeman, B. J.; Regev, O. *Zeolites* **1996**, *17*, 447.
(15) Twomey, T. A. M.; Mackay, M.; Kuipers, H. P. C. E.; Thompson, R. W. *Zeolites* **1994**, *14*, 162.
(16) Dokter, W. H.; van Garderen, H. F.; Beelen, T. P. M.; van Santen, R. A.; Bras, W. *Angew. Chem., Int. Ed. Engl.* **1995**, *34*, 73.

10.1021/cm0200689 CCC: $22.00
Published on Web 05/15/2002

Preparation of macrocrystals using nanocrystals as building blocks is attractive because of the relatively easy control of the properties of the nanoscale modules.[1] Although the aggregation pathways of the nanocrystals have been extensively studied in several systems,[3,5,6,11,16] little is known about the energetics involved.

In this study we use an in situ calorimetric method to follow the heat effect associated with the crystal growth of pure silica TPA-MFI zeolite from an initially clear solution. The composition of the synthesis solution and its preparation procedure are the same as or comparable to those in earlier experiments in the literature.[4−16] This permits us to correlate our new results with the previous studies. Our objectives are to investigate the energy evolution of the synthesis system during the course of crystal growth and to delineate the interplay between thermodynamic factors and changes in the solution chemistry and interface properties. The new results presented here complement the previous synthesis investigations by providing direct experimental evidence of the fundamental forces governing the synthesis events. They also extend our earlier work on the energetics of various high silica zeolite structures studied using high-temperature oxide melt solution calorimetry.[17,18]

Experimental Section

Preparation of the Initial Synthesis Solution. The synthesis mixture with the composition $9.00TPAOH-25.0SiO_2-480.0H_2O-100.0C_2H_5OH$ was prepared as reported by Schoeman.[4] 119.10 g of 10% TPAOH solution (Fisher), 30.32 g of 40% TPAOH solution (Alfa), and 68.40 g of tetraethyl orthosilicate (TEOS: Alfa, 99.9%) were mixed under vigorous stirring at room temperature (25 °C). All agents were used as received. The TEOS phase and the aqueous TPAOH solution were initially not completely miscible and formed an emulsion-like mixture under stirring. After about 2−3 h of reaction (under stirring), the mixture became a homogeneous and completely clear solution to the naked eye. After about 6 h of stirring, the mixture was stored at 0 °C for further use.

In situ Synthesis and Calorimetric Measurement. A Calvet-type heat flow microcalorimeter (Setaram C80) was used as reported previously.[19−21] The calorimeter was operated isothermally at 95.15 ± 0.01 °C. The initial synthesis mixture (7.50 g) was placed in a Teflon-lined stainless steel vessel for the in situ synthesis and calorimetric measurement. The same amount of water (7.5 g) was used as reference because its heat content is close to that of the synthesis system. The synthesis reaction was timed from the moment the sample vessel was loaded into the calorimeter. The loading causes a significant disturbance to the calorimeter. Blank experiments (using water as both sample and reference) show that it takes more than 2 h for the calorimeter to re-establish its baseline. Thus, meaningful calorimetric data can only be collected after 2 h. The energy equivalent of the calorimetric signal was calibrated electrically and checked by using the melting enthalpies of indium and naphthalene.[21] We note here that the calorimeter chamber is essentially at constant volume. Moreover, below the boiling point of the solution, there is little, if any, change in pressure during synthesis. Throughout the rest of this paper, we use the terms "enthalpy", "energy", and "energetics" essentially interchangeably, because the difference between ΔE and ΔH is negligible.

Collection of the TPA-MFI Nanocrystals. After a predetermined time of heating at 95.15 °C, the vessel was pulled out of the calorimeter, and the reaction was immediately quenched in cold water. After equilibrating to room temperature (25 ± 1 °C), the vessel was opened and the pH of the mixture was measured. As-synthesized solid product was collected by centrifugation. A Beckman L8-80 M ultracentrifuge with a 70-Ti rotor operated at 30 000 rpm, giving a relative centrifugal force of 66 000 g, was used. The solid fraction was separated from the mother liquor after 2 h of centrifugation. The solid particles were redispersed in deionized water and centrifuged again. The washing and centrifugation procedure was typically repeated four times. At the end of the procedure, the pH value of the liquid is below 9. The washed solid was dried in air (calorimeter lab area: 25 ± 1 °C and 50 ± 3% relative humidity) for at least 7 days. The centrifugation tube containing the dry solid was weighed to determine the yield of the synthesis.

Characterization Techniques. The crystal structure of the solid product was examined by its powder X-ray diffraction (XRD) pattern recorded on an Inel XRG 3000 diffractometer (Ni-filtered Cu Kα radiation, 30 kV, 30 mA). The resolution of the position-sensitive detector is $2\theta = 0.029°$. The particle size and morphology of the zeolite crystals were analyzed using a high-resolution scanning electron microscope (FEI XL30 SFEG). The water and organic contents of the solid product were determined by thermogravimetric analysis linked with differential scanning calorimetry (TGA-DSC, Netzsch STA 449 C Jupiter) in flowing oxygen, 40 mL/min. The heating rate was 10 °C/min. The pH value of the synthesis mixture was measured using an Ag/AgCl Sure-Flow Electrode (Thermo Orion, Model 91-72BN). Every time before use, the electrode was calibrated using two standard buffer solutions (pH = 7.0 and 10.0).

Results

In Situ Synthesis, Calorimetry, and Characterization. A heat flow curve associated with the in situ synthesis events is presented in Figure 1 (curve ϕ_0). After the thermal disturbance caused by loading the vessels, a flat segment (t = 2.5 h → 6.5 h) indicates negligible thermal events occurring. The synthesis mixture remains clear, and no solid can be recovered by centrifugation. Therefore, the heat flow curve during this period is taken as the initial baseline for the thermal peaks which follow.

At $t_1 = 6.64 \pm 0.17$ (13) h (the error represents two standard deviations of the mean; the value in parentheses denotes the number of repeated experiments), the onset of an exothermic peak is discerned. At $t_2 = 11.22 \pm 0.16$ (7) h, an exothermic maximum is reached. Thereafter, the exothermic event rapidly changes into a relatively more pronounced endothermic event. At $t_3 = 11.89 \pm 0.21$ (5) h, the heat flow curve crosses the baseline (taken as the extension of the initial baseline) from exothermic to endothermic. At $t_4 = 12.39 \pm 0.21$ (4) h, a sharp endothermic peak is seen. At $t \approx 16$ h, the calorimetric curve flattens and remains flat for at least 5 more days. Thereafter, the synthesis is complete at 16 h and the following flat curve is the final baseline for the preceding thermal peaks. This conclusion is also supported by both the constant solid yield and constant pH of the synthesis mixture thereafter (see below). On the basis of the deviations of t_1, t_2, t_3, and t_4, we estimate the error ±0.20 h for positioning the synthesis time using an in situ calorimetric trace.

(17) Piccione, P. M.; Laberty, C.; Yang, S.; Camblor, M. A.; Navrotsky, A.; Davis, M. E. *J. Phys. Chem. B* **2000**, *104*, 10001.
(18) Petrovic, I.; Navrotsky, A.; Davis, M. E.; Zones, S. I. *Chem. Mater.* **1993**, *5*, 1805.
(19) Yang, S.; Navrotsky, A.; Phillips, B. L. *J. Phys. Chem. B* **2000**, *104*, 6071.
(20) Yang, S.; Navrotsky, A.; Phillips, B. L. *Microporous Mesoporous Mater.* **2001**, *46*, 137.
(21) Yang, S.; Navrotsky, A. *Microporous Mesoporous Mater.* **2002**, *52*, 93.

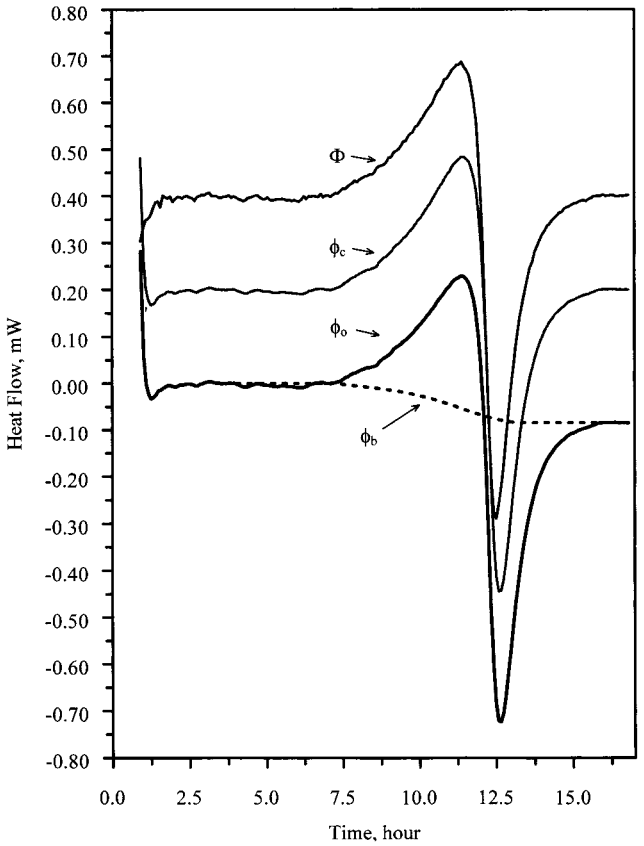

Figure 1. Heat flow curves of in situ synthesis from 7.50 g of 9.00TPAOH−25.0SiO_2−480.0H_2O−100.0C_2H_5OH at 95.15 °C: ϕ_0, recorded curve on a Setaram C80 calorimeter; ϕ_b, constructed baseline based on mass of solid product; ϕ_c, corrected curve after subtracting ϕ_b from ϕ_0; Φ, true heat flow curve restored from ϕ_c (see text for details). Note that, for clarity, ϕ_c and Φ are moved upward by 0.20 and 0.40 mW, respectively.

In Figure 1 the final baseline of the ϕ_0 curve is slightly shifted to the endothermic direction from the level of the initial baseline. From our experience, the baseline is very sensitive to the geometry of the sample in the vessel. Within the time span of the thermal peaks (7−16 h), the clear solution becomes more and more turbid and then, near the end of this period, the TPA-MFI crystals settle and a clear supernatant emerges. Thus, we infer that the small baseline shift reflects the change in the synthesis mixture from single phase to multiphase. Following this rationale, we corrected the small baseline shift on the basis of the mass change of the MFI-TPA crystals (see quantitative data of the TPA-MFI crystal mass as a function of reaction time in Figure 5). ϕ_b and ϕ_c in Figure 1 represent the constructed baseline and the heat flow curve after baseline correction. In any even, the baseline correction is small, and the final results are relatively insensitive to the details of how it is made.

Because of the time constant (τ) of the calorimeter response to thermal perturbation, the true heat flow curve (Φ) is different from the observed calorimetric signal.[20,21] However, the τ value under the conditions of this study, 6.464 ± 0.046 min, is very small relative to the time span of the heat flow peaks (several hours). Therefore, Φ can be accurately recovered from the recorded heat flow curve (ϕ) using the following equation

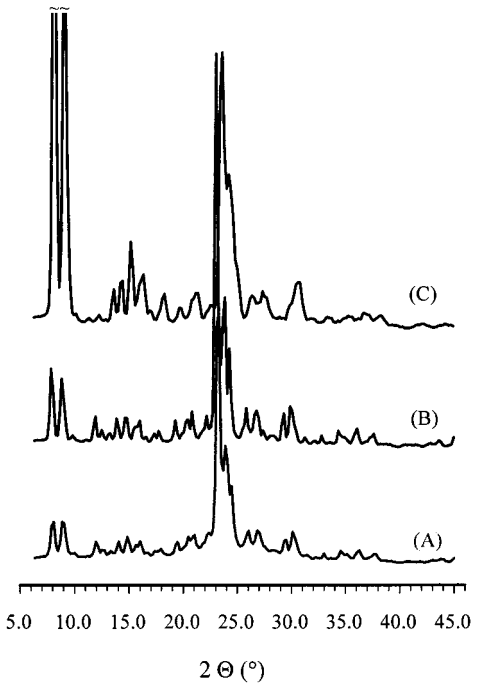

Figure 2. XRD patterns of the solid products collected from the in situ synthesis 9.00TPAOH−25.0SiO_2−480.0H_2O−100.0C_2H_5OH: (A) after 8.1 h of synthesis at 95.15 °C; (B) after 110 h of synthesis at 95.15 °C; (C) after calcination of the sample from part B at 550 °C for 2 h.

$$\Phi(t) = \phi(t) + \tau\frac{d\phi(t)}{dt} \quad (1)$$

Details about how to derive this equation, to determine its applicability, and to correctly measure τ have been reported elsewhere.[21] The recovered Φ is presented in Figure 1. The integration of the Φ peaks (ΔH_{total}) over the entire period of crystal growth gives 0.38 ± 0.05 J, corresponding to the total enthalpy change of the crystal growth reaction from 7.5 g of the synthesis solution.

The onset of the thermal peak at t = 6.64 ± 0.17 h coincides with the time at which the clear synthesis mixture turns to a murky suspension. From that time on, solid product can be collected by centrifugation. The XRD profiles confirm that the solid products formed throughout the thermal peaks are pure TPA-MFI phases because neither additional peaks due to other crystalline phase(s) nor X-ray baseline humps due to amorphous components are present (Figure 2). Even after a prolonged reaction time of reaction (t = 110 h), the solid product remains pure TPA-MFI. After removal of TPA species in the as-synthesized TPA-MFI crystals by thermal treatment at 550 °C in air for 2 h, the XRD results indicate that the MFI structure remains intact (Figure 2).

The TPA-MFI products under SEM appear as discrete particles with a relatively narrow size distribution (Figure 3). The average particle size increases as the synthesis proceeds; for example, at t = 8.1 h, the diameter is about 40−60 nm, and at t > 16 h, it is about 80−120 nm. After calcination, however, the discrete character of the crystals is lost and a relatively large and irregular sheetlike form is seen, which is indicative of coarsening during calcination (Figure 3). The TGA-DSC analysis shows that the TPA-MFI crystals lose 15.6% of their mass when heated to 800 °C at 10 °C/

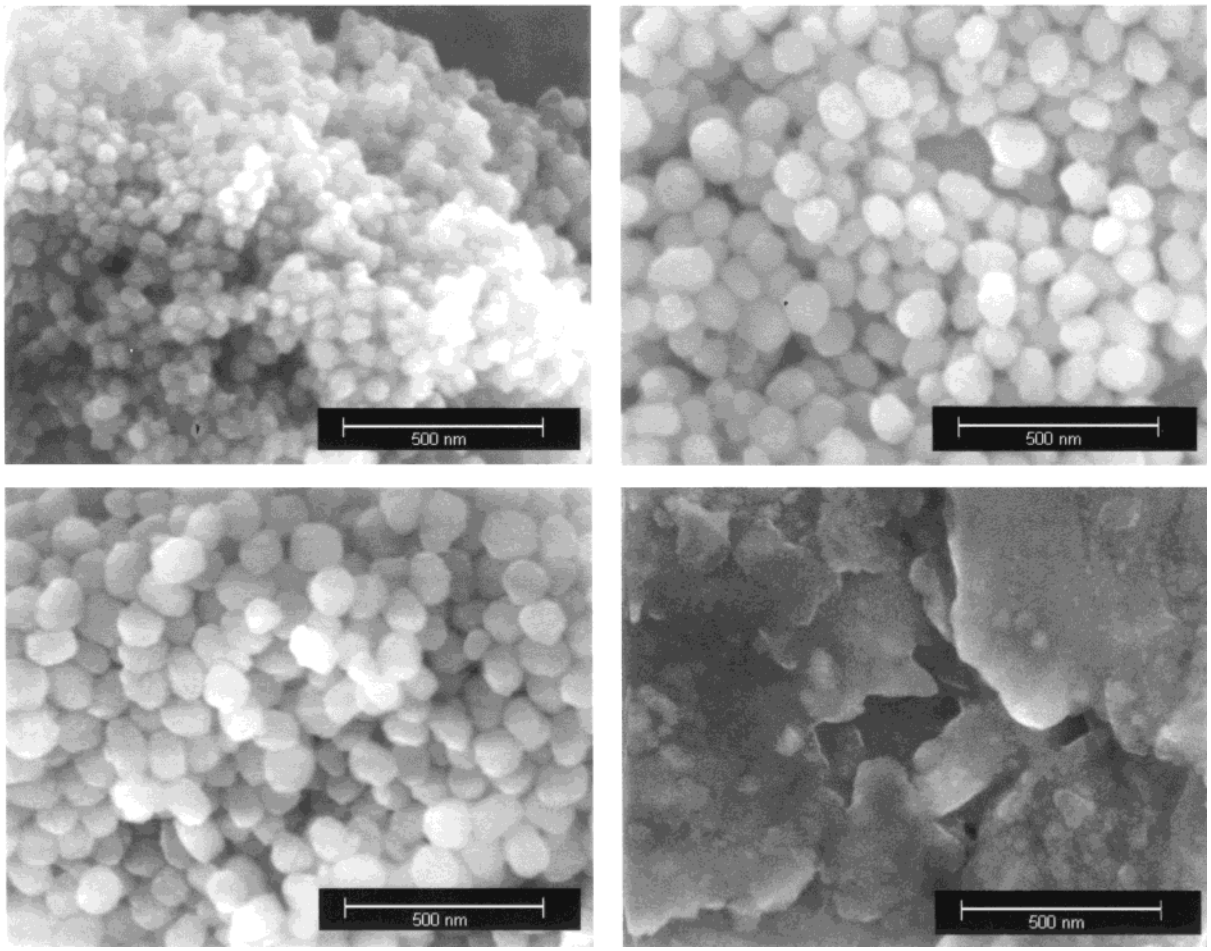

Figure 3. SEM photos of the solid products collected from the in situ synthesis 9.00TPAOH−25.0SiO_2−480.0H_2O−100.0C_2H_5-OH at 95.15 °C: after 8.1 h (top left); after 12.5 h (top right); after 110 h (bottom left); after 110 h and calcination in air at 550 °C for 2 h (bottom right).

min under oxygen flow (Figure 4). The mass loss is attributed to water desorption, desorption and combustion of TPAOH molecules and TPA ions, and dehydroxylation of the terminal silanol groups.[10,22] The SiO_2 content of the TPA-MFI crystals is 84.4 wt %.

Mass of TPA-MFI Crystals and Change of Integral Enthalpy as a Function of Time. To investigate the synthesis chemistry associated with the thermal peaks, a series of repeated in situ syntheses were terminated after various preselected reaction times. The crystal mass (M) and the corresponding change of the integral enthalpy (ΔH_{int}) based on Φ are plotted as a function of reaction time (see the insets in Figures 5 and 6, respectively). The errors in M and ΔH_{int} are estimated on the basis of their deviation in the repeated measurements. The ΔH_{int} data for $t < 12$ h and M data for $t < 12.7$ h can be satisfactorily fitted by the following power equation,

$$\Delta H_{int} \text{ or } M = k(t - t_0)^n \qquad (2)$$

where t_0 stands for the starting time, n for the order of the time dependence, and k for the rate constant. The fitting results are listed in Table 1. Clearly the mass of the collected TPA-MFI increases monotonically throughout both the exothermic and endothermic periods.

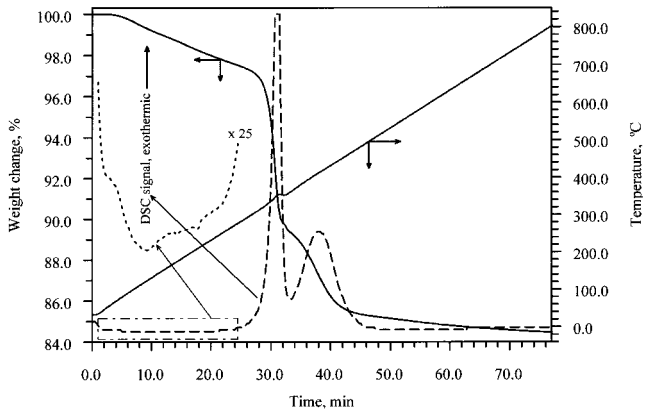

Figure 4. TG-DSC profiles of the TPA-MFI crystals with the scanning rate 10 °C/min and oxygen gas flow 40 mL/min. The upward direction of the DSC signal indicates an exothermic effect. The sample is collected from the in situ synthesis at 95.15 °C after 110 h.

Monitoring the pH Changes. After preparation of the synthesis mixture at room temperature but before heating in the calorimeter, its pH is 12.5−12.6. After 11.4 h of in situ synthesis at 95.15 °C, the pH remains essentially the same within experimental error, indicating negligible variation of OH^- activity (and concentration) in solution (see Figure 7). The errors of the pH measurements are estimated on the basis of the scatter of the readings during the measurements. This scatter

(22) Soulard, M.; Bilger, S.; Kessler, H.; Guth, J. L. *Zeolites* **1987**, *7*, 463.

Table 1. Fitting Equations and Results for the Mass of the Collected TPA-MFI Crystals (M, mg) as a Function of Time (t, h), the Change of the Integrated Enthalpy (ΔH_{int}, J) as a Function of t, and ΔH_{int} as a Function of M in the in Situ Synthesis from 7.50 g of 9.00TPAOH−25.0SiO_2−480.0H_2O−100.0C_2H_5OH at 95.15 °C

fitting equation	data range	results
$M = k_{M_0}(t - t_{M_0})^{n_M}$	8.1 h < t < 12.7 h	$n_M = 2.92 \pm 0.34$; $t_{M_0} = 4.48 \pm 0.77$ h; $k_M = 1.06 \pm 0.97$ mg/h
$\Delta H = k_{H_0}(t - t_{H_0})^{n_H}$	8.1 h < t < 11.5 h	$n_H = 3.10 \pm 0.03$; $t_{H_0} = 6.22 \pm 0.04$ h; $k_H = -0.012 \pm 0.001$ J/h
$\Delta H = kM + c$	40 mg < M < 300 mg	$k = -0.0072 \pm 0.0002$ J/mg; $c = 0.34 \pm 0.04$ J

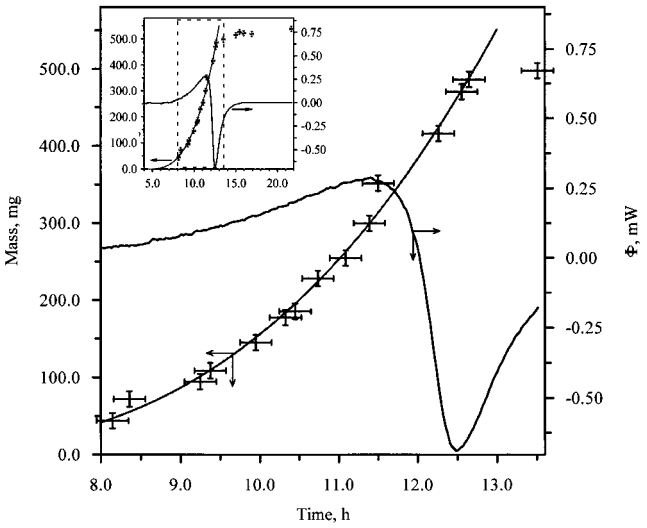

Figure 5. Mass of the collected TPA-MFI crystals in the in situ synthesis from 7.50 g of 9.00TPAOH−25.0SiO_2−480.0H_2O−100.0C_2H_5OH at 95.15 °C. Note that the fit is based on the data t < 13 h (see also Table 1).

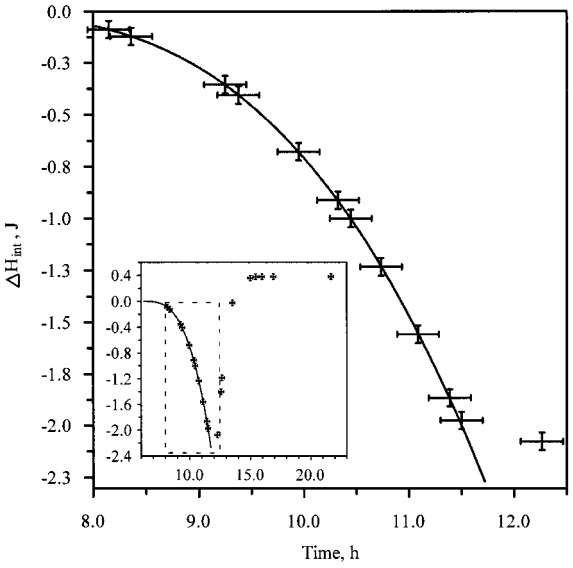

Figure 6. Change of the integrated enthalpy (ΔH_{int}) in the in situ synthesis from 7.50 g of 9.00TPAOH−25.0SiO_2−480.0H_2O−100.0C_2H_5OH at 95.15 °C. Note that the fit is based on the data t < 11.7 h (see also Table 1).

is considerably larger than the precision (0.01) specified by the manufacturer mainly because the synthesis mixture has a very high alkalinity whose pH is known to be very difficult to measure accurately. After 11.4 h of synthesis, a rapid rise in pH is observed, coinciding with the rapid thermal switch from exothermic to endothermic. After about 16 h of synthesis, the pH value is stabilized again but to a new level at about 13.25−13.35, which also coincides with the end of the endothermic peak. For reference, we also prepared a solution with the same composition as that of the synthesis mixture but without the silica component (i.e., 9.00TPAOH−480.0H_2O−100.0C_2H_5OH).[23] The pH of this solution is higher than 14 (the pH meter is not readable when pH > 14), and this is expected, since the hydroxide concentration of this solution is about 2.0 M. The lower pH of the synthesis solution is thus considered with adsorption of OH^- on the particle surfaces.

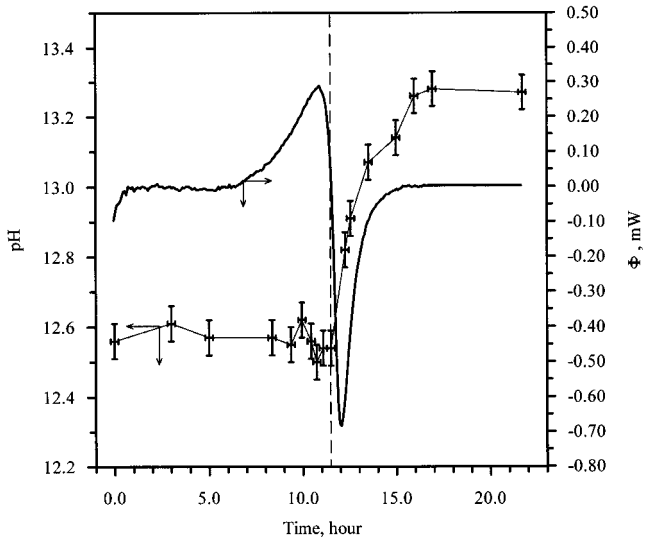

Figure 7. Synthesis solution pH as a function of time in the in situ synthesis from 9.00TPAOH−25.0SiO_2−480.0H_2O−100.0C_2H_5OH at 95.15 °C. Note that the pH measurements were carried out at 25 °C after quenching the synthesis mixture to room temperature. For reference, the heat flow curve of the in situ synthesis is also shown in the figure.

Clearly, the silica in the highly alkaline synthesis mixture, acting as acid, neutralizes much of the strong base [OH^-] in the solution. The neutralization reaction proceeds by hydrolyzing silica to form hydroxyl groups [≡Si−OH] and consuming free [OH^-] via deprotonation. A pH-buffered effect appears in the early period of the synthesis (t < 11.4 h). This buffer region persists even after considerable crystal growth has occurred. The end of the buffer region (Figure 7) is marked by the exo → endo thermal switch, corresponding to about 65% completion of the synthesis (based on the mass of the TPA-MFI crystals).

Two Stages of Crystal Growth. The nearly monodisperse TPA-MFI crystals shown in Figure 3 indicate that no additional nuclei are formed during crystal growth. The n_M value obtained by fitting (Table 1) is very close to the theoretical value of 3 corresponding to linear growth ($L \propto t$ because $M \propto L^3$ and $M \propto t^3$, where L stands for the average diameter of the crystals). Linear crystal growth in the synthesis of silica TPA-MFI zeolite has been well documented in the literature.[4,11,12,15] The results in Figures 5 and 6 and Table 1

(23) 9.07 g of 40% TPAOH solution was diluted with 11.70 g of DI water. To this solution was added 9.14 g of ethanol, and the final solution was homogenized by stirring.

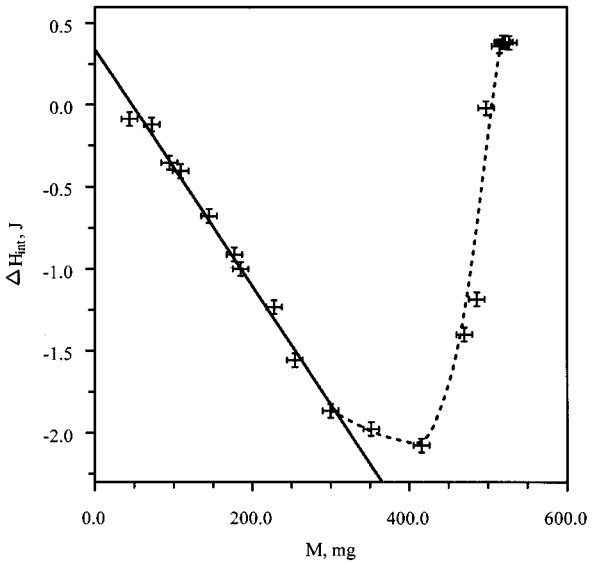

Figure 8. Change of the integrated enthalpy (ΔH_{int}) vs the mass (M) of the collected TPA-MFI crystals in the in situ synthesis from 7.50 g of 9.00TPAOH−25.0SiO_2−480.0H_2O−100.0C_2H_5OH at 95.15 °C. Note that the linear fit is based on the data with M < 350 mg (see also Table 1).

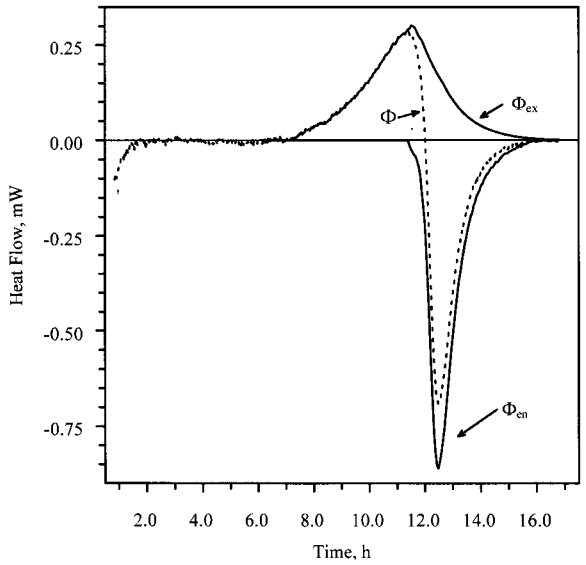

Figure 9. Exothermic component (Φ_{ex}) and endothermic component (Φ_{en}) of the heat flow curve (Φ) obtained in the in situ synthesis calorimetry of 7.50 g of 9.00TPAOH−25.0SiO_2−480.0H_2O−100.0C_2H_5OH at 95.15 °C.

imply that ΔH_{int} runs parallel to M. This correspondence is clearly shown by the linearity between ΔH_{int} and M in the period t < 11.5 h (see Figure 8). The starting time (t_0) of the linear crystal growth period is 6.2 h on the basis of ΔH_{int} or 4.5 h on the basis of M. The former (t_0 = 6.2 h) is probably more reliable because ΔH_{int} can be measured more accurately than M. Indeed, the fit based on ΔH_{int} is better, as seen by comparing Figures 5 and 6.

From eq 2 and the parameters listed in Table 1, the estimated M and the associated ΔH_{int} at the onset of the exothermic peak (6.64 h) are 10 mg and −1 μJ, respectively. One microjoule is below the detection limit of the present calorimetric method. The small mass is near the errors of the experimental procedure and corresponds to a yield of less than 2% (assuming 100% at the end of the reaction). However, the crystal size corresponding to 10 mg of mass is already about 30 nm in diameter. Therefore, both the M and ΔH_{int} data presented in this study cover the principal crystal growth region but not nucleation and very early crystal growth.

The linear relationship between ΔH_{int} and M (Figure 8), and the nearly constant pH value (Figure 7) in the exothermic period of crystal growth together suggest a "steady state" or "buffered state" of the batchwise synthesis reaction. Apparently, the accumulated chemical changes associated with the crystal growth have negligible effect on the kinetic behavior of further crystal growth (implications will be discussed further). Our data also show, however, that this steady state cannot be sustained when the exo → endo thermal switch takes place ($t \approx$ 11.5 h). Using the established $\Delta H_{int} \sim M$ linearity at t < 11.5 h, we can investigate the deviation of the heat flow behavior during the non-steady state at t > 11.5 h. Φ_{ex} in Figure 9 represents the hypothetical heat flow curve if the steady state of the synthesis reaction was maintained throughout the synthesis. At $t \leq$ 11.5 h, Φ_{ex} equals Φ, and at t > 11.5 h, it is calculated on the basis of M and the established linear relationship between ΔH_{int} and M, that is, using the following equation,

$$\Phi_{ex} \equiv \frac{d\Delta H_{int}}{dt} = k\frac{dM(t)}{dt} \qquad (3)$$

Φ_{en} in Figure 9 represents the heat flow deviation of the actual synthesis reaction from Φ_{ex}, that is, $\Phi_{en} = \Phi - \Phi_{ex}$. The integration of the Φ_{ex} peak (ΔH_{ex}) gives −3.39 ± 0.05 J, corresponding to the total enthalpy change if the crystal growth reaction from 7.5 g of the synthesis solution proceeded only in the steady state mode. The integration of the Φ_{en} peak (ΔH_{en}) gives 3.77 ± 0.05 J, corresponding to the deviation of the actually measured enthalpy change (ΔH_{total}) from ΔH_{ex}, that is, $\Delta H_{en} = \Delta H_{total} - \Delta H_{ex}$. It should be pointed out that Φ_{ex} at t > 11.5 h is only approximate because of the limited number of M data, the experimental errors, and the amplified uncertainty because of differentiating the integral-type M data. On the other hand, Φ_{en} is less affected by the uncertainty of Φ_{ex} because the contribution of the experimentally measured Φ is much greater than that of Φ_{ex} shortly after t = 11.5 h (Figure 9). The ΔH_{ex} and ΔH_{en} calculations are not affected by the uncertainty in Φ_{ex} because they are directly calculated from the final mass data.

Discussion

Thermodynamic Aspects of Crystal Growth. In situ calorimetry provides, for the first time, direct evidence of an exo → endo thermal switch during the course of growing TPA-MFI crystals. The thermal switch (centered at t =11.5 h, see Figure 9) divides two stages of crystal growth. Stage-I is a steady state characterized by exothermic enthalpy, linear crystal growth rate, constant pH, and constant ratio between the integral enthalpy change and crystal mass ($\Delta H_{int}/M$). Stage-II is a non-steady state with an endothermic reaction, an increasingly less-than-linear crystal growth rate, a rapid rise in pH, and a sharp change in the $\Delta H_{int}/M$ ratio.

The variation of ΔH_{int} with the extent of crystal growth can be evaluated from the slope of the $\Delta H_{int}-M$ curve in Figure 8 by defining $\Delta H' = d\Delta H_{int}/dM$. Throughout stage-I, $\Delta H'$ is constant, -0.514 ± 0.014 kJ/mol of SiO_2, indicating a constant energetic driving force for the crystal growth reaction. In stage-II, the driving force diminishes and an increasingly large energetic hindering force quickly follows. $\Delta H'$ is roughly 2.5 kJ/mol of SiO_2 near the end of stage-II. The positive $\Delta H'$ value is intriguing for two reasons. First, the crystal growth seems to proceed uphill in the energetic landscape of the system evolution. Second, a relatively stronger entropy driving force must be present to surpass the energetic dragging force. The derivative of the entropy with the extent of crystal growth ($\Delta S' = d\Delta S_{int}/dM$, per mole of SiO_2) is about 7 J/(mol of SiO_2·K) near the end of the crystallization period, since the reaction is very close to thermodynamic equilibrium then; that is, $\Delta G' \approx 0$ (see further discussion below).

The obtained $\Delta H'$ arises from the collective heat effect of all the chemical events associated with the crystal growth, including breaking/forming chemical bonds when the interface is eliminated by crystal growth, release of H_2O and/or OH^- from the eliminated interface into bulk solution and the corresponding variation of the bulk solution chemistry (e.g., dilution and/or solvation), and changes in the properties of the remaining interface in response to the variation of the bulk solution chemistry. Previous investigation by high-temperature oxide melt calorimetry showed that the formation enthalpy of many silica zeolitic structures and amorphous silica is within a range of only 7 kJ/mol of SiO_2.[17,18] The magnitude of $\Delta H'$ obtained in this study is comparable to the energetic differences among silica zeolitic polymorphs. However, at present, it is not possible to quantify the contributions of these events and further studies in this direction are underway.

The increase of $\Delta S'$ may be attributed mainly to the release of the small chemical species (H_2O and/or OH^-) from the eliminated interface into solution.[3] The final volume of the TPA-MFI crystals is less than 4% of the initial solution volume. The volume of the released water from the eliminated surface should be very small relative to the volume of the mother liquor. The dilution effect on pH is thus negligible within the errors of pH measurements.

Solution Chemistry and Surface Charge Density. The profile of the pH changes in this study is similar to that for the syntheses of silica TPA-MFI involving amorphous gels.[24−26] The pH rise in those syntheses is mainly attributed to the depletion of the amorphous phase near the end of crystallization. Since amorphous material is absent throughout our synthesis, the pH change obviously arises from different chemical causes.

Extensive synthesis studies of silica TPA-MFI zeolite from initially clear solutions by different research groups have demonstrated the presence of preassembled primary particles (PPs) throughout the synthesis.[4−16] The PPs are about 3 nm in diameter, and their population decreases during crystallization.[4−6,11,16] The crystal growth at elevated temperatures proceeds by aligned addition or oriented attachment of PPs to the growing crystals, although intermediate particles, about 7−10 nm in diameter, also formed from PPs, may also be involved in the nucleation and crystal growth.[5−7]

Since the PPs have closely similar compositional and structural features to those of the final TPA-MFI crystals, the electrical double layer (EDL) properties of their interfaces with the synthesis mother liquor are presumably similar.[27] The TPA-MFI crystal growth from PPs could be visualized as the decrease of the overall surface of the solid particles (or crystal−aqueous solution interface). The eliminated surface caused by crystal growth must expel the surface charges through two possible pathways. One is by compressing the surface charges onto the remaining surface via further deprotonation of the silanols there. The other is by releasing OH^- into solution. The latter pathway will raise the pH of the mother liquor, but the former will not.

In stage-I the elimination of the interface by crystal growth does not release net hydroxide groups into the solution (or the released hydroxide groups are readsorbed onto the remaining interface) because of the constant pH in this period (Figure 7). The surface charge density or the surface $\equiv Si-O^-/\equiv Si-OH$ ratio must increase by increasing the degree of deprotonation of the surface silanols. Apparently, the increase of surface $\equiv Si-O^-/\equiv Si-OH$ ratio is not energetically hindered and the enthalpy of crystallization, per mole of SiO_2, remains constant. In stage-II the sharp rise of the solution pH and rapid change of $\Delta H'$ from exothermic to endothermic demonstrate that a further increase of the surface $\equiv Si-O^-/\equiv Si-OH$ ratio becomes energetically unfavorable relative to the release of the OH^- into solution. Clearly, different pathways of discharging the eliminated interface are involved during different stages of crystal growth. The increasing energy associated with increasing surface charge density appears to control the pathway.

The energetic cause for the variation of the surface $\equiv Si-O^-/\equiv Si-OH$ ratio and the related pH buffer effect in solution may be qualitatively analyzed as follows. First, it is well established that deprotonation reactions of silicate monomers or silicate oligomers may proceed in multiple steps as the pH increases.[28] A pH buffer effect may be expected; for example, $H_2SiO_4^{2-}/H_3SiO_4^-$ forms a buffer system at pH $\approx$ 12.3.[29]By analogy, the silicate surfaces (of the TPA-MFI crystals and PPs) may have similar pH buffer effects depending on the surface $\equiv Si-O^-/\equiv Si-OH$ ratio. We infer that, when the surface charge density is higher than some critical value, for example, perhaps when one $\equiv Si-O^-$ begins to have an adjacent $\equiv Si-O^-$, a nonlinear sudden shift to the endothermic direction occurs to hinder further increase of the surface charge density. Second, the negatively charged surfaces are stabilized by the presence of counterions in the proximity of the surface to form the electrical double layer. In the present synthesis solution,

(24) Fegan, S. G.; Lowe, B. M. *J. Chem. Soc., Faraday Trans. 1* **1986**, *82*, 785.
(25) Lowe, B. M. *Zeolites* **1983**, *3*, 300.
(26) Casci, J. L.; Lowe, B. M. *Zeolites* **1983**, *3*, 186.
(27) Sverjensky, D. A.; Sahai, N. *Geochim. Cosmochim. Acta* **1998**, *62*, 3703.
(28) Sefcik, J.; McCormick, A. V. *AIChE J.* **1997**, *43*, 2773.
(29) Derived using the equilibium constants of the monomer silicate deprotonation: $pK_1 = 9.5$, $pK_2 = 12.6$, $pK_3 = 15.7$, and $pK_4 = 18.8$ (see Table 1 of ref 28).

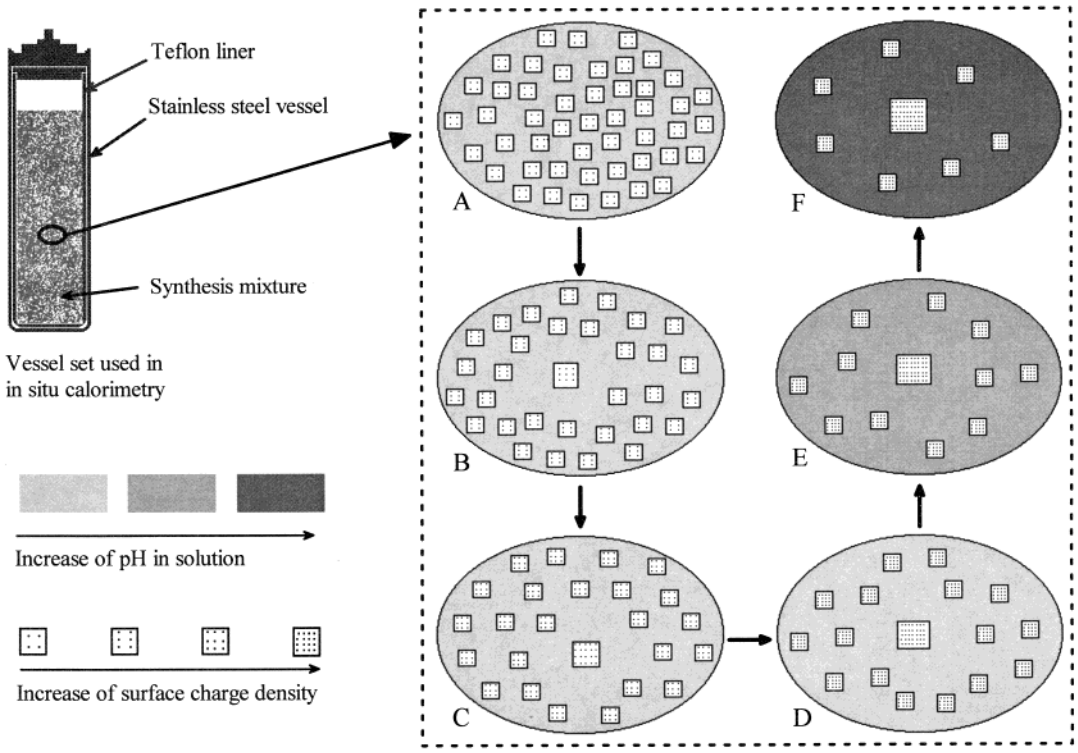

Figure 10. Schematic representation of growing silica TPA-MFI crystals by aligned aggregation of the preassembled primary particles: stage-I, A → B → C → D, with increase of surface charge density but not the solution pH; stage-II, D → E → F, with increase of the solution pH but not the surface charge density.

TPA^+ ions are the only cations ($[H^+]$ is negligible at high pH). Because of the bulky size, we infer that TPA^+ ions in the first sorption shell interact more effectively with the surface charges than those in the second layer. When the surface ≡Si−O^-/≡Si−OH ratio or the surface charge density increases, more TPA^+ ions will be drawn to the first shell. But when the first shell is saturated, a further increase of the ≡Si−O^-/≡Si−OH ratio may be encountered with an abrupt and nonlinear enthalpy change to the endothermic direction. This will make the other pathway (i.e., releasing OH^- into solution) prevail.

The results of this study demonstrate that lowering the total interface between the particles and the mother liquor via crystal growth can alter the interface properties and/or the solution chemistry, which in turn influence the dynamics of further crystal growth. Such a feedback loop of crystal growth is significant because of the small size and large specific surface area of the particles involved. The surface charge density of silica is known to be significantly influenced by the structure of the silica, the nature and concentration of the cations, and any cosolvent.[30−32] To understand and control the crystal growth behavior in preparation of zeolitic materials such as membranes and large single crystals,[33−38] detailed information on how the local structure and the aggregation reactivity of the crystal surface response to the variation of the surface charge density and solution chemistry is highly desirable. However, to our knowledge, few studies on the surface charge density of silica zeolites, especially in the pH range relevant to the synthesis systems, have been undertaken.

Mechanistic Implications. The following mechanism of TPA-MFI crystal growth emerges from our results and discussion (see Figure 10). In stage-I (steps A → B → C → D in Figure 10), the crystal growth proceeds steadily and linearly by the incorporation of PPs. The eliminated surfaces/interfaces release OH^- ions into solution. Since the pH does not rise, one can infer that, at the same time, the remaining surfaces adsorb an equal number of OH^- ions from solution. The net effect is that the surface charge is compressed onto the remaining surfaces and no net the OH^- is transferred between the surface and the solution. In addition, the release of water molecules into the solution increases the entropy of the system. However, not enough H_2O is released to dilute the solution and lower its pH. Both $\Delta H'$ and $\Delta S'$ are driving forces for crystal growth in this stage. In stage-II (steps D → E → F in Figure 10), the crystal growth still proceeds by the incorporation of PPs but with a diminishing reaction rate (Figure 5). The pH of the mother liquor increases rapidly because the elimination of the interface by crystal growth expels net OH^- (and water molecules) into the solution. There is no significant change of the surface charge density because of the energetic barrier. $\Delta S'$

(30) Rodrigues, F. A.; Monteiro, P. J. M.; Sposito, G. *Cem. Concr. Res.* **1999**, *29*, 527.
(31) Rodrigues, F. A.; Monteiro, P. J. M.; Sposito, G. *J. Colloid Interface Sci.* **1999**, *211*, 408.
(32) Rudzinski, W.; Piasecki, W.; Panas, G.; Charmas, R. *J. Colloid Interface Sci.* **2000**, *226*, 353.
(33) Tsapatsis, M.; Xomeritakis, G.; Hillhouse, H.; Nair, S.; Nikolakis, V.; Bonilla, G.; Lai, Z. *CATTECH* **2000**, *3*, 148.
(34) Wang, Z.; Yan, Y. *Chem. Mater.* **2001**, *13*, 1101.
(35) Qiu, S.; Yu, J.; Zhu, G.; Terasaki, O.; Nozue, Y.; Pang, W.; Xu, R. *Microporous Mesoporous Mater.* **1998**, *21*, 245.
(36) Wu, C. N.; Chao, K. J.; Tsai, T. G.; Chiou, Y. H.; Shih, H. C. *Adv. Mater.* (*Weinheim, Ger.*) **1996**, *8*, 1008.
(37) Metzger, T. H.; Mintova, S.; Bein, T. *Microporous Mesoporous Mater.* **2001**, *43*, 191.
(38) Wang, Z.; Yan, Y. *Microporous Mesoporous Mater.* **2001**, *48*, 229.

remains a driving force for the crystal growth in this stage. But $\Delta H'$ evolves from a driving force to an increasingly hindering force.

PPs remain in the mother liquor at the end of crystal growth.[4,6,7] Chemical extraction experiments suggest that more than 80% of the silica initially present in the clear solution is converted to PPs.[9] The total crystallization in this study corresponds to a yield less than 70%. Therefore, the end of crystal growth is not due to the depletion of all PPs but rather to the increasingly positive $\Delta H'$ term, which can no longer be offset by the $T\Delta S'$ term. $\Delta S'$ is expected to be relatively constant toward the end of crystallization because on a unit mass basis of the formed zeolite crystals the amount of water and/or hydroxide ions released from the eliminated surface is constant. The rate of the linear crystal growth in stage-I is affected neither by the continuous decrease of the PP population nor by the initial PP population.[11] This independence is consistent with kinetic control of the crystal growth by surface reaction, for example, aligning the PPs that are initially anchored on the growing crystals so that the minimum energy orientation may be achieved. Our results in Figure 5 suggest that the linear crystal growth may extend somewhat into stage-II, where the reaction is already significantly endothermic. This observation may be explained as follows. At the early part of stage-II, even though the reaction is increasingly energetically hindered, the entropic driving force may keep $\Delta G'$ sufficient negative so that the crystal growth remains kinetically controlled in the same manner as in stage-I. That is, the reverse reaction (dissociation of the large crystals into PPs) remains insignificant. This argument is reasonable because each PP has hundreds of SiO_2 units and the magnitude of the thermodynamic energy is much larger than the thermal energy (3 kJ/mol at the reaction temperature). Upon further crystal growth, the reaction rate levels off because thermodynamic control gradually prevails over kinetic control.

The findings of this study may have more general implications. Other systems, for example, TiO_2 and $BaTiO_3$, have been prepared to grow from aqueous solution by aggregation of colloidal particles analogous to the PPs invoked for zeolites.[39−41] The balance between particle growth and surface charge elimination may lead to analogous energetic and kinetic behavior in these and other oxide and oxyhydroxide systems. Reactions in cement chemistry may be subject to similar constraints. The concepts proposed here should be tested by combined calorimetric, analytical, structural, and computational studies in a wide variety of systems.

Conclusions

The crystal growth of silica TPA-MFI zeolite from an initial clear solution is divided into two stages by a distinct exo → endo thermal switch associated with the reaction. In the exothermic stage, the linear crystal growth is driven by a constant energetic driving force, -0.514 ± 0.014 kJ/mol of SiO_2. In this period, the solution pH is buffered by the alteration of surface (interface) charge density. In the endothermic stage, the enthalpy evolves from a driving force into a hindering force, about 2.5 kJ/mol near the end of the stage. Crystal growth under the energetic hindering force implies an entropic driving force, which is mainly attributed to the liberation of small chemical species such as OH^- and/or H_2O into solution from the eliminated interface. In contrast to the case of the exothermic stage, the surface charge density in this period is buffered by variation of the solution pH. The strong correlation between the thermal switch and the change in the buffer effect suggests that the evolution of the chemical events during the crystal growth is primarily governed by the associated enthalpy changes.

Acknowledgment. We thank Michael Dunlap for his assistance with the SEM analysis. We acknowledge the National Science Foundation for financial support (Grants DMR-97-31782 and DMR-01-01391).

CM0200689

(39) Lee, T.; Yao, N.; Imai, H.; Aksay, I. A. *Langmuir* **2001**, *17*, 7656.
(40) Lee, T.; Yao, N.; Aksay, I. A. *Langmuir* **1997**, *13*, 3866.
(41) Penn, R. L.; Banfield, J. F. *Science* (*Washington, D. C.*) **1998**, *281*, 969.